European Journal of Radiology Open 5 (2018) 87–91

Contents lists available at ScienceDirect

European Journal of Radiology Open

journal homepage: www.elsevier.com/locate/ejro

Feasibility of Macrophage Plaque Imaging Using Novel Ultrasmall Superparamagnetic Iron Oxide in Dual Energy CT

Hideyuki Sato[a,b], Shinichiro Fujimoto[a,*], Yosuke Kogure[c], Hiroyuki Daida[a]

[a] Department of Cardiovascular Medicine, Juntendo University Graduate School of Medicine, Tokyo, Japan
[b] Department of Radiology, Edogawa Hospital, Tokyo, Japan
[c] Department of Radiology, Juntendo University Hospital, Tokyo, Japan

ARTICLE INFO

Keywords:
ultrasmall superparamagnetic iron oxide
plaque imaging
dual energy CT
macrophage

ABSTRACT

Purpose: While ultrasmall superparamagnetic iron oxide (USPIO) is useful for identifying atherosclerotic lesions as an MRI contrast medium, there are limitations in its power to quantitatively evaluate and resolve USPIO in atherosclerotic lesions of the heart. Computed tomography (CT) has a higher resolution than MRI, and Dual Energy CT is capable of visualizing iron atoms, the main component of USPIO. More recently, a new USPIO capable of achieving longer retention times in blood circulation compared to the previous USPIO has been developed. The objective of this study was to investigate the feasibility of visualizing and quantifying the new USPIO by dual energy CT.

Materials and Methods: USPIO with iron concentrations adjusted in 5 steps from 2.5 to 50 mg/mL was visualized by dual energy CT to measure the contrast on virtual monochromatic imaging (40 and 70 keV). In parallel experiments, iodine contrast medium was diluted to the same concentrations and visualized by dual energy CT to measure the contrast at 70 keV. The linearity of the contrast against the iron and iodine concentrations was measured for the quantitative evaluation. Further, a vascular phantom simulating clinical cases (divided into 4 layers: meat alone, meat + USPIO, vascular lumen, and with or without calcification) was prepared. The iron density image was overlaid on the image at 70 keV to evaluate the visualization of the USPIO medium.

Results: In the imaging of the medium with an iron concentration of 25 mg/mL, the CT numberat 70 keV was 117.0 HU, or about 17% of that of iodine (664.4 HU). The CT number rose to 319.9 HU at 40 keV, or to about 48% of that of iodine. The linearity of the contrast against the iron concentration in USPIO was $R^2 = 0.9996$, indicating a strong correlation. In the simulated vascular phantom, the iron concentration significantly increased in the region containing USPIO, and the quantity could be visualized by overlaying the iron density image displayed with a color scale on the 70-keV image.

Conclusion: Our results suggested that macrophages could be both quantified and visualized by USPIO on dual energy CT.

1. Introduction

No method has been established to predict and prevent the onset of acute coronary syndrome, a set of symptoms that develop suddenly without forewarning [1]. Given that the chief pathology of acute coronary syndrome is thrombotic occlusion, the problem may be largely solvable through the accurate identification of vulnerable plaque, that is, plaque that induces thrombotic occlusion at a high rate. Vulnerable plaque causing rupture, the cause of acute coronary syndrome in about 60% of cases, is one of the most important targets [2]. Vulnerable plaque is characterized by thin fibrous caps (thinner than 65 μm) and positive remodeling, as well as the presence of abundant oxidatively modified low density lipoprotein and macrophages [3–5]. While vulnerable plaque can be identified noninvasively by imaging the coronary artery using coronary CT angiography and coronary MR angiography [6–8], but problems remain with the objectivity, quantitative, and diagnostic performance of those techniques. Inflammation also provides valuable diagnostic information by dint of its important actions in destabilizing plaque [9], but no molecular imaging method capable of evaluating inflammation has been established in a clinical setting.

Ultrasmall superparamagnetic iron oxide (USPIO) is retained in the blood circulation for a long time because of the very small size of the

Abbreviations: CCTA, coronary computed tomographic angiography; DECT, dual energy computed tomography; USPIO, ultrasmall superparamagnetic iron oxide; CMEADM, carboxymethyl-diethylaminoethyl dextran magnetite ultrasmall superparamagnetic iron oxide; VMI, virtual monochromatic image; MDI, material density image

* Corresponding author at: Department of Cardiovascular Medicine, Juntendo University Graduate School of Medicine, 2-1-1 Hongo, Bunkyo-ku, Tokyo 113-8421, Japan.
E-mail address: s-fujimo@tj8.so-net.ne.jp (S. Fujimoto).

https://doi.org/10.1016/j.ejro.2018.05.003
Received 27 June 2017; Received in revised form 4 May 2018; Accepted 5 May 2018
Available online 15 May 2018

particles that compose it (about 50 nm), and the medium is also unlikely to be incorporated by Kupffer cells in the liver. The accumulation of USPIO in macrophages in atherosclerotic lesions has been confirmed in studies using MRI [10,11]. Researchers have also developed carboxymethyl-diethylaminoethyl dextran magnetite USPIO (CMEADM-U, The Nagoya Research Laboratory Meito Sangyo, Aichi, Japan), a new USPIO that remains within the blood circulation for longer than the original USPIO [12]. While CMEADM-U holds strong potential, two factors limit its effective use for the evaluation of the coronary artery: the inferior resolution of MRI versus CT and the challenges in quantitative evaluation. Dual energy CT (DECT) is now capable of both preparing a virtual monochromatic image (VMI) and acquiring a material density image (MDI) in a clinical setting [13,14]. Images can be acquired at a specifically changed effective energy using VMIs, and the contrast can be freely changed after the VMIs are obtained. Specific substances can now be emphasized or suppressed in the MDIs acquired. Virtual non-contrast images can be obtained from water/(iodine) images prepared by suppressing the iodine component of contrast imaging using iodine contrast medium and acquiring water/(fat) images with the fat component suppressed and iron/(water) images with the iron component emphasized. Meanwhile, the iron content can also be measured by setting a region of interest (ROI) in the target region.

Our group speculates that it may be possible to visualize the macrophages present in coronary arterial lesions using USPIO to quantitatively evaluate the lesions by preparing MDIs of iron, the main component of USPIO, from DECT images. In this study we investigated the feasibility of imaging and evaluating USPIO using DECT.

2. Materials and Methods

CMEADM-U was used as the USPIO contrast medium in our experiments. Some of the hydroxyl groups in CMEADM-U are substituted by carboxyl and diethyl amino groups (Fig. 1). As a consequence, the medium is retained in the blood for a shorter period than the original USPIO medium [12].

2.1. Quantitative evaluation using dilute contrast medium

Lots (φ30 mm) of CMEADM-U adjusted to 5 iron concentrations, 2.5, 5, 10, 25, and 50 mg/mL, were placed in an acrylic phantom (φ200 mm) and visualized by DECT against a background filled with water (Fig. 2). Similarly, iodine contrast medium was diluted at the same dilution rate and visualized by DECT under the same conditions. In the VMI, the effective energy was changed and the CT number was measured at 70 keV (corresponding to 120 kVp) and 40 keV. The coefficient of determination (R^2) was calculated to evaluate the correlation between the dilution concentration and CT number. In parallel, iron/(water) images scaled against the iron density values on the MDIs were prepared to measure the iron content (mgFe/cm^3).

2.2. Evaluation of visualization using simulated blood vessels

A simulated vascular phantom (Fuyo Corporation, Tokyo, Japan) divided into 4 layers (meat alone, meat + CMEADM-U, vascular lumen, and with or without calcification) (Fig. 3) was placed in an acrylic phantom (φ200 mm) and visualized by DECT. Table 1 shows the composition of each layer. The iron concentration of the CMEADM-U was set in 3 steps, namely, 5, 25, and 50 mg/mL, and the background was filled with water. An earlier study reported an accumulation of USPIO in plaque on imaging at 24 or more hours after administration of the medium [11]. The simulated vascular phantom in the present study was therefore prepared on the assumption that the CMEADM-U accumulated only in regions in which macrophages were present. Regarding the acquisition of images after 24 hours, the CMEADM-U was assumed to be fully washed from the phantom, leaving none remaining in the vascular lumen. Meanwhile, a phantom with the vascular lumen filled with iodine contrast medium was also prepared to allow us to simultaneously determine the stenosis rate of the coronary artery and evaluate the plaque based on CMEADM-U by intravenously administering iodine contrast medium and acquiring CCTA images at the same time.

Color scale maps of images were prepared by plotting the iron and water contents on the vertical and horizontal axes, respectively using a Gemstone Spectral Imaging (GSI) scatter plot and overlaid on a 70-keV VMI on the display (Fig. 4).

2.3. Acquisition conditions

The X-ray CT images were taken using a Discovery CT750 HD system (CT750, GE healthcare, Milwaukee, USA). The CT750 allows the use of a fast kV switching-mode DECT in which dual energy data can be acquired by rapidly switching between 140 and 80 kVp during a single rotation of the X-ray tube [14]. The acquisition conditions were as follows: tube voltage, 140 kVp/80 kVp; tube current, 600 mA; tube rotation time, 1.0 s; acquisition mode, axial scan; slice thickness, 0.625 mm; slice interval, 0.625 mm; matrix, 512 × 512; Recon kernel, Standard. The images were analyzed using a Gemstone Spectral

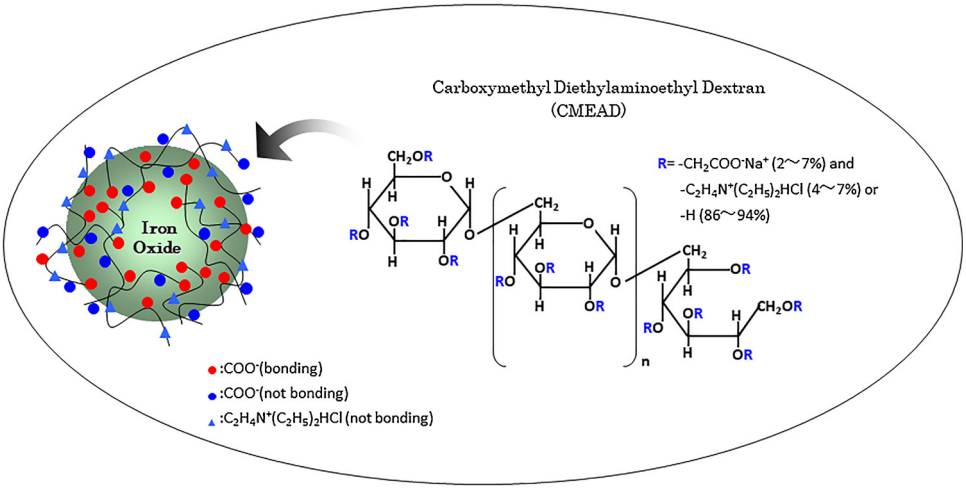

Fig. 1. Composition of Carboxymethyl-diethylaminoethyl Dextran Magnetite USPIO.
USPIO: Ultrasmall Superparamagnetic Iron Oxide.

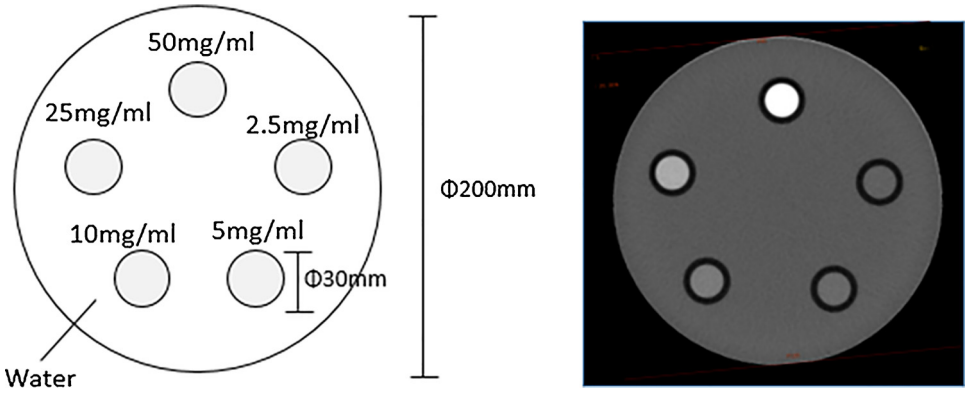

Fig. 2. Dilute contrast medium phantom.

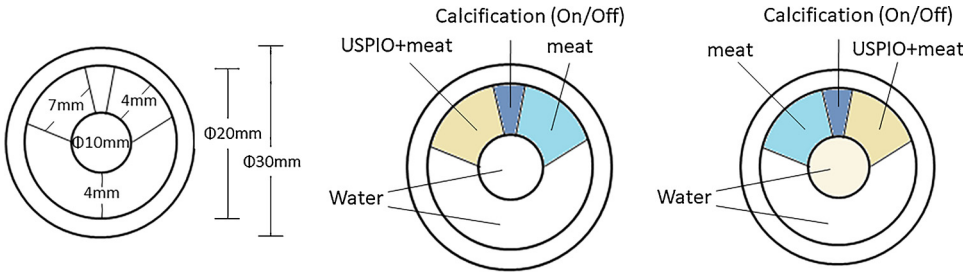

Fig. 3. Simulated vascular phantom.
A simulated vascular phantomdivided into 4 layers (meat alone, meat + Carboxymethyl-diethylaminoethyl Dextran Magnetite USPIO, vascular lumen, and with or without calcification) was prepared, placed in an acrylic phantom. The iron concentration in Carboxymethyl-diethylaminoethyl Dextran Magnetite USPIO was set to 3 steps: 5, 25, and 50 mg/mL.
USPIO: Ultrasmall Superparamagnetic Iron Oxide.

Table 1
The component of simulated blood vessel phantom.

Rot	USPIO (mgFe/ml)	Calcification	Meat (g)	Meat +USPIO (g)	Percentage of USPIO (%)
1 (a)	5	-	1.14	1. 03	18. 10*
2 (b)	25	+	0. 88	1. 00	18. 10**
3 (c)	50	-	1. 10	1. 03	18. 10***
4 (d)	5	+	0. 84	1. 00	18. 10*
5 (e)	25	-	1. 14	1. 03	18. 10**
6 (f)	50	+	0. 91	1. 01	18. 10***

* We mixed meat 4.20 g and USPIO 0.93 g and made it.
** We mixed meat 4.08 g and USPIO 0.90 g and made it.
*** We mixed meat 4.25 g and USPIO 0.94 g and made it.

Imaging Application for the Advantage Workstation Volume Share5 (AW, GE Healthcare, Milwaukee, USA).

3. Results

3.1. Feasibility of quantitative evaluation using diluted contrast medium

Table 2 shows the relationships between the CT numbers and dilution concentrations of each contrast medium. The CT number of CMEADM-U increased as the iron concentration rose. At an effective energy of 70 keV, a level at which a CT number similar to that at 120 kVp on conventional CT is reached, the CT numbers of 2.5 and 50 mg Fe/mL were 12 and 240.8 HU, respectively. The linear approximation line was y = 4.8x and R^2 was 0.9996, showing a strong correlation. By changing the effective energy to 40 keV, the CT numbers of 2.5 and 50 mgFe/mL increased to 25.9 and 671.1 HU, respectively. The linear approximation line was y = 13.3x and R^2 was 0.9993, showing a strong correlation in spite of the reduction of the effective energy to 40 keV. Regarding the iodine contrast medium, the CT numbers at the 2.5 and 50 mgI/mL concentrations were 60.1 and 1186.0 HU, respectively. The linear approximation line was y = 24.3x, showing high CT numbers, and R^2 was 0.9957, showing a strong correlation.

In the iron content measurements using MDIs, the concentrations at 2.5, 5.0, 10, 25 and 50 mgFe/mL were 1.6, 4.2, 9.0, 22.4 and 47.3 mgFe/cm^3, respectively (Table 2).

3.2. Evaluation of visualization using the simulated vascular phantom

When the ROI was set in the region in which CMEADM-U and meat were mixed, the iron content levels measured using MDIs were

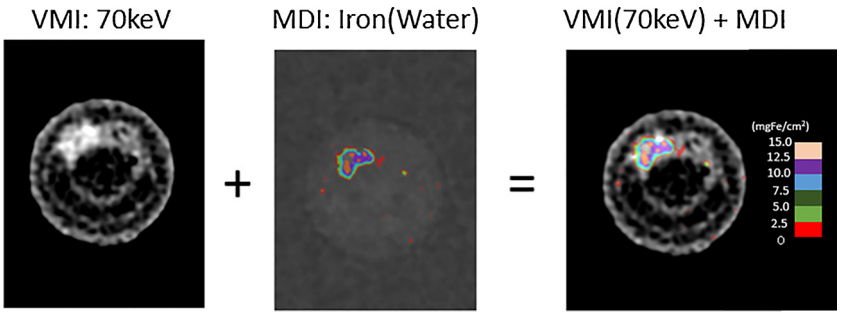

Fig. 4. Method of overlay map of VMI and MDI.
We displayed the color map at 2.5 mgFe/ml intervalsVMI: Virtual Monochromatic Imaging, MDI: Material Density Imaging.

Table 2
Table shows vary and correlation of the contrast for the iron / iodine concentration.

Iron / iodine concentration (mg/ml)	2. 5	5. 0	10. 0	25. 0	50. 0	R^2
DECT, Iron content measurement value (CMEADM-U, mgFe/mm^3)	1. 6	4. 2	9. 0	22. 4	47. 3	-
CT number (CMEADM-U, 70 keV, HU)	12. 0	25. 6	48. 8	117. 0	240. 8	0. 9996
CT number (CMEADM-U, 40 keV, HU)	25. 9	68. 7	132. 8	319. 9	671. 1	0. 9993
CT number (Iodine, HU)	60. 1	120. 1	241. 4	664. 4	1186. 0	0. 9957

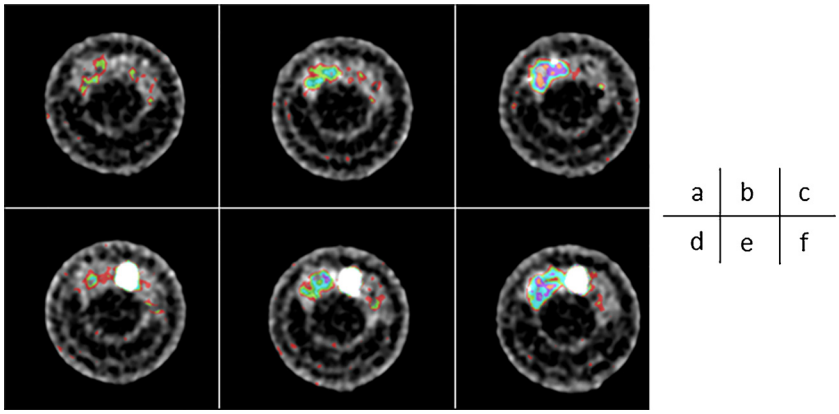

Fig. 5. Over lay map of VMI and MDI in simulated vascular phantom.
(a) The iron concentration was 5mgFe/ml, without calcification (HAP), (b) The iron concentration was 25mgFe/ml, without calcification (HAP), (c) The iron concentration was 50mgFe/ml, without calcification (HAP), (d) The iron concentration was 5mgFe/ml, with calcification (HAP), (e) The iron concentration was 25mgFe/ml, with calcification (HAP), (d) The iron concentration was 50mgFe/ml, with calcification (HAP). The presence of calcification in the lesion did not influence the findings (a < b < c, d < e < f).
VMI: Virtual Monochromatic Imaging, MDI: Material Density Imaging.

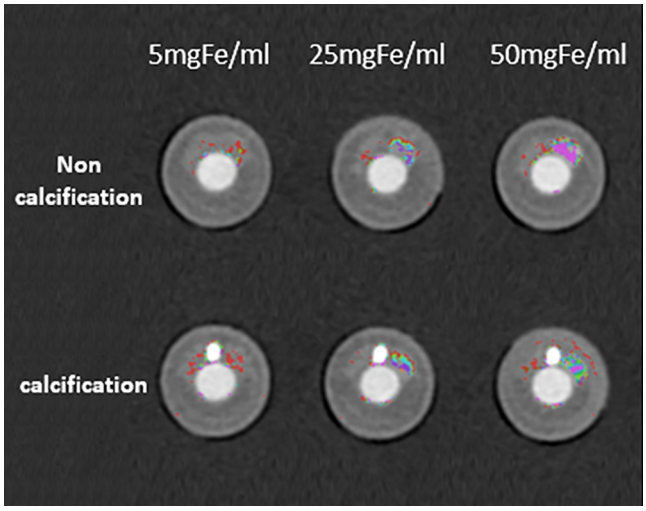

Fig. 6. Simulate vascular phantom filled with iodine contrast medium.
Influence of the iodine contrast medium on Carboxymethyl-diethylaminoethyl Dextran Magnetite USPIO accumulation was not shown.
USPIO: Ultrasmall Superparamagnetic Iron Oxide.

1.8 ± 1.6, 6.2 ± 0.9, and 14.1 ± 1.0 mgFe/cm^3 in the 10-, 25-, and 50-mgFe/mL lots, respectively. Color scale maps prepared to set the iron content to 0-20 mgFe/cm^3 (2.5 steps) were overlaid on the 70-keV images on the display. The CMEADM-U accumulation could be visually evaluated on the resulting images (Fig. 5a–c). The presence of calcification in the lesion had no influence on the findings (Fig. 5d–f). Similar findings were obtained in the phantom in which the vascular lumen was filled with iodine contrast medium, showing no influence of the iodine contrast medium on CMEADM-U accumulation (Fig. 6).

4. Discussion

In this study we used a DECT imaging modality to investigate the feasibility of quantifying and visualizing CMEADM-U, a USPIO contrast medium with a long retention time in blood circulation. We began by changing the dilution rate of CMEADM-and evaluating its correlation with the contrast achieved. A strong correlation was noted even though the effective energy of the VMI was changed, suggesting that a quantitative evaluation was possible. The contrast of CMEADM-U, however, was only about 50% of that of iodine contrast medium even at 40 keV, the level at which contrast on the VMIs reached maximum. The target CT number of a coronary artery CTA using iodine contrast medium is about 350 HU, and the medium is administered at a fractional dose of about 20 mgI/kg/sec. If CMEADM-U used on a coronary artery CTA was to acquire a contrast equivalent to that provided by the current iodine contrast medium, it would be have to be administered at a fractional dose of about 40 mgFe/kg/sec, a level clinically difficult to achieve. There would be no need for fast infusion, however, if the CMEADM-U was used only to evaluate the plaque formed by phagocytosis by macrophages. In that scenario, a preferable form of administration might be intravenous injection or drip infusion of the CMEADM-U after sufficient time was allowed for the macrophages to phagocytose the medium. The newly developed CMEADM-U, with its longer retention time in blood than the previous USPIO, may also be very useful in this regard.

The main component of CMEADM-U is iron. We investigated the feasibility of quantitatively evaluating the iron content using DECT-based MDId. Quantitative evaluation using DECT has been reported in several earlier studies. Xian et al. measured the iron content in the liver using DECT for comparison with the levels measured on MRI [15]. The iron content measured using MDIs deviated from the true value at a low concentration. Under the acquisition conditions in our study, the standard deviation of background noise was 2.2, suggesting that noise influenced the value measured on the MDI. In the 10-, 25-, and 50-mgFe/mL lots, the deviation from the true value was less than 10%, and the value measured on the MDI generally rose as the concentration increased, supporting the feasibility of iron content measurement by the MDI. A method using iterative reconstruction to reduce noise on CT has been proposed and clinically applied [16,17]. If a similar technique becomes applicable for MDIs in the future, background noise may be resolved and values closer to the true values may be obtained.

We prepared conditions simulating actual coronary atherosclerotic lesions using a vascular phantom to investigate differences in the distribution of CMEADM-U under variable conditions. In comparing the distribution of CMEADM-U distribution under conditions with and without calcification, the presence of calcification near the plaque had no marked influence on the distribution, supporting the feasibility of

evaluation. A technology to inhibit the beam-hardening effect in DECT largely eliminates the influence of surrounding substances, an important cause of reduced accuracy in CT numbers. This beam-hardening effect is also effective for MDIs, which leads us to believe that calcification may have had no effect on the iron-density-based iron/(water) images in our study. In parallel experiments we performed a simultaneous CCTA evaluation of vascular lumen filled with iodine contrast medium. The MDI turned out to be unaffected by the presence of iodine contrast medium nearby, which told us that it was possible to simultaneously perform a CCTA evaluation with iodine contrast medium while recording contrast images of the plaque with CMEADM-U. When we added contrast medium adjusted to 5, 25, and 50 mgFe/mL into the simulated vascular phantom, the actual accumulation decreased. We prepared the phantom by mixing CMEADM-U and meat with an iron content of -0.6 ± 0.8 mgFe/cm^3 in the meat region, and created images based on two materials, iron and water, in the MDI. The meat (fat) visualized with the two-material modality was negative. The meat:CMEADM-U ratio was about 4:1, suggesting that the admixture with meat diluted the iron concentration. Accumulation was marked at 50 mgFe/mL, and local regions with high accumulation were also clearly visualized. Lipids and fibers are abundant in the background of coronary artery plaque in clinical cases, predicting the occurrence of similar dilutions. If, however, the plaque incorporates CMEADM-U to some extent, DECT-based imaging may be possible. Our experiments also showed an increase in sensitivity at the high CMEADM-U concentration of 50 mgFe/mL.

We investigated the feasibility of visualizing and quantifying CMEADM-U by DECT using a dilution phantom and simulated vascular phantom. We prepared a vascular phantom simulating plaque containing macrophages by mixing contrast medium and meat. The meat, however, was surrounding by a coating of contrast medium in the phantom, creating a condition inconsistent with the mechanism by which the macrophages present in atherosclerotic lesions of the human body phagocytose the iron (CMEADM-U) freely present in the blood vessels. An evaluation of the coronary arteries also requires an understanding of the influences of both the ECG triggered/gated mechanism and the motion artifacts due to a high heart rate. Evaluation under conditions closer to clinical cases may be necessary. More can also be done to clarify the accumulation of the USPIO contrast medium. While MRI findings have clearly shown that USPIO accumulates in plaque, the degree of accumulation relative to the dose remains unknown. By administering CMEADM-U to animals with atherosclerotic lesions in a future study, we could explore whether the macrophages incorporate CMEADM-U in systemic circulation or if similar findings can be obtained.

5. Conclusion

Our findings suggested that CMEADM-U imaging by dual energy CT may be useful for visualizing and quantifying macrophage accumulation in plaque. We expect this technology to emerge as a new modality for imaging coronary arterial plaque.

Disclosures

Dr. Daida has received research funds from Kyowa Hakko Kirin Company Ltd., Philips Electronics Japan, Ltd. Astellas Pharma Inc., ABBOTT JAPAN CO., Ltd., Sanofi K.K., Eisai Co., Ltd., Shionogi & Co., Ltd., Daiichi-Sankyo Company, Ltd., Dainippon Sumitomo Pharma Co., Ltd., Takeda Pharmaceutical Co., Ltd., Nippon Boehringer Ingelheim Co., Ltd., Bayer Yakuhin, Ltd., Pfizer Co., Ltd., Philips Electronics Japan, Ltd., TOSHIBA MEDICAL SYSTEMS CORPORATION, FUJIFILM Corporation, Bristol-Myers Squibb Company, Boston Scientific Japan K.K., SANWA KAGAKU KENKYUSHO Co., Ltd., MSD.K.K., and endowed department from ResMed Japan K.K. Philips Electronics Japan, Ltd., Fukuda Denshi Co., Ltd. TOSHIBA MEDHICAL SYSTEMS are unrelated to this project.

Funding sources

This research did not receive any specific grant from funding agencies in the public, commercial, or not-for-profit sectors.

Conflicts of interest

None.

References

[1] E. Braunwaald, Epilogue: What Do Clinicians Expect From Imagers? JACC 47 (2006) 101–103.
[2] M. Naghavi, P. Libby, E. Falk, S.W. Casscells, S. Litovsky, J. Rumberger, J.J. Badimon, C. Stefanadis, P. Moreno, G. Pasterkamp, Z. Fayad, P.H. Stone, S. Waxman, P. Raggi, M. Madjid, A. Zarrabi, A. Burke, C. Yuan, P.J. Fitzgerald, D.S. Siscovick, C.L. de Korte, M. Aikawa, K.E. Juhani Airaksinen, G. Assmann, C.R. Becker, J.H. Chesebro, A. Farb, Z.S. Galis, C. Jackson, I.K. Jang, W. Koenig, R.A. Lodder, K. March, J. Demirovic, M. Navab, S.G. Priori, M.D. Rekhter, R. Bahr, S.M. Grundy, R. Mehran, A. Colomb, E. Boerwinkle, C. Ballantyne, W. Insull Jr., R.S. Schwartz, R. Vogel, P.W. Serruys, G.K. Hansson, D.P. Faxon, S. Kaul, H. Drexler, P. Greenland, J.E. Muller, R. Virmani, P.M. Ridker, D.P. Zipes, P.K. Shah, J.T. Willerson, From vulnerable plaque to vulnerable patient: a call for new definitions and risk assessment strategies; Part I, Circulation 108 (2003) 1664–1672.
[3] A.P. Burke, A. Farb, G.T. Malcom, Y.H. Liang, J. Smialek, R. Virmani, Coronary risk factors and plaque morphology in men with coronary disease who died suddenly, N Engl J Med. 336 (1997) 1276–1282.
[4] H.C. Stary, A.B. Chandler, R.E. Dinsmore, V. Fuster, S. Glagov, W. Jr, M.E. Insull, C.J. Rosenfeld, W.D. Schwartz, R.W. Wagner, Wissler, A definition of advanced types of atherosclerotic lesions and a histological classification of atherosclerosis. A report from the committee on vascular lesions of the council on arteriosclerosis, American heart association, Arteriosclerosis, Thrombosis Vasc Biol 15 (1995) 1512–1531.
[5] J. Narula, A.V. Finn, A.N. Demaria, Picking plaques that pop, J Am Coll Cardiol. 45 (2005) 1970–1973.
[6] S. Motoyama, M. Sarai, H. Harigaya, H. Anno, K. Inoue, T. Hara, H. Naruse, J. Ishii, H. Hishida, N.D. Wong, R. Virmani, T. Kondo, Y. Ozaki, J. Narula, Computed tomographic angiography characteristics of atherosclerotic plaques subsequently resulting in acute coronary syndrome, J Am Coll Cardiol. 54 (2009) 49–57.
[7] S. Motoyama, H. Ito, M. Sarai, T. Kondo, H. Kawai, Y. Nagahara, H. Harigaya, S. Kan, H. Anno, H. Takahashi, H. Naruse, J. Ishii, H. Hecht, L.J. Shaw, Y. Ozaki, J. Narula, Plaque characterization by coronary computed tomography angiography and the likelihood of acute coronary events in mid-term Follow-Up, J Am Coll Cardiol. 66 (2015) 337–346.
[8] T. Noguchi, T. Kawasaki, A. Tanaka, S. Yasuda, Y. Goto, M. Ishihara, K. Nishimura, Y. Miyamoto, K. Node, N. Koga, High-intensity signals in coronary plaques on noncontrast T1-weighted magnetic resonance imaging as a novel determinant of coronary events, J Am Coll Cardiol. 63 (2014) 989–999.
[9] P. Libby, Inflammation in atherosclerosis, Nature 420 (2002) 868–874.
[10] S.G. Ruehm, C. Corot, P. Vogt, S. Kolb, J.F. Debatin, Magnetic resonance imaging of atherosclerotic plaque with ultrasmall superparamagnetic particles of iron oxide in hyperlipidemic rabbits, Circulation 103 (2001) 415–422.
[11] C. Corot, K.G. Petry, R. Trivedi, A. Saleh, C. Jonkmanns, J.F. Le Bas, E. Blezer, M. Rausch, B. Brochet, P. Foster-Gareau, D. Balériaux, S. Gaillard, V. Dousset, Macrophage imaging in central nervous system and in carotid atherosclerotic plaque using ultrasmall superparamagnetic iron oxide in magnetic resonance imaging, Invest Radiol. 39 (2004) 619–625.
[12] N. Nitta, K. Tsuchiya, A. Sonoda, S. Ota, N. Ushio, M. Takahashi, K. Murata, S. Nohara, Negatively charged superparamagnetic iron oxide nanoparticles: a new blood-pooling magnetic resonance contrast agent, Jpn J Radiol 30 (2012) 832–839.
[13] L. Yu, S. Leng, C.H. McCollough, Dual-energy CT-based monochromatic imaging, AJR Am J Roentgenol. 199 (2012) S9–S15.
[14] C.H. McCollough, S. Leng, L. Yu, J.G. Fletcher, Dual- and multi-energy CT: Principles, technical approaches, and clinical applications, Radiology 276 (2015) 637–653.
[15] X.F. Luo, X.Q. Xie, S. Cheng, Y. Yang, J. Yan, H. Zhang, W.M. Chai, B. Schmidt, F.H. Yan, Dual-energy CT for patients suspected of having liver iron overload: Can virtual iron content imaging accurately quantify liver iron Content? Radiology 277 (2015) 95–103.
[16] T. Nakaura, S. Nakamura, N. Maruyama, Y. Funama, K. Awai, K. Harada, S. Uemura, Y. Yamashita, Low contrast agent and radiation dose protocol for hepatic dynamic CT of thin adults at 256-detector row CT: effect of low tube voltage and hybrid iterative reconstruction algorithm on image quality, Radiology 264 (2012) 445–454.
[17] Z. Deal, J.M. Grimm, M. Treiti, L.L. Geyer, U. Linsenmaier, M. Korner, M.F. Reiser, S. Wirth, Filtered back projection, adaptive statistical iterative reconstruction, and a model-based iterative reconstruction in abdominal CT: an experimental clinical study, Radiology 266 (2013) 197–206.